American Journal of Internal Medicine
2019; 7(4): 102-111
http://www.sciencepublishinggroup.com/j/ajim
doi: 10.11648/j.ajim.20190704.14
ISSN: 2330-4316 (Print); ISSN: 2330-4324 (Online)

Impact of Integrated Whole Body ^{68}Ga PET/MR Imaging in Comparison with ^{68}Ga PET/CT in Lesions Detection and Diagnosis of Suspected Neuroendocrine Tumours

Alshaima Alshammari[1], Michael Masoomi[1, *], Rizwan Syed[2], Evangelia Skoura[3], Sofia Michopoulou[2], Fulvio Zaccagna[4], Jamshed Bomanji[2], Francesco Fraioli[2]

[1]Nuclear Medicine Department, Adan Hospital, Kuwait City, Kuwait

[2]Institute of Nuclear Medicine, University College London Hospitals, London, UK

[3]PET/CT Department, Bioiatriki Hospital, Athens, Greece

[4]School of Clinical Medicine, University of Cambridge, Cambridge, UK

Email address:

Alshaima_97@hotmail.com (A. Alshammari), masoomim@sky.com (M. Masoomi), riz999@hotmail.com (R. Syed), iskoura@yahoo.com (E. Skoura), sofiamichopoulou@googlemail.com (S. Michopoulou), fz247@cam.ac.uk (F. Zaccagna), jamshed.bomanji@nhs.net (J. Bomanji), fraioli.francesco@gmail.com (F. Fraioli)

[*]Corresponding author

To cite this article:

Alshaima Alshammari, Michael Masoomi, Rizwan Syed, Evangelia Skoura, Sofia Michopoulou, Fulvio Zaccagna, Jamshed Bomanji, Francesco Fraioli. Impact of Integrated Whole Body ^{68}Ga PET/MR Imaging in Comparison with ^{68}Ga PET/CT in Lesions Detection and Diagnosis of Suspected Neuroendocrine Tumours. *American Journal of Internal Medicine*. Vol. 7, No. 4, 2019, pp. 102-111.
doi: 10.11648/j.ajim.20190704.14

Received: June 26, 2019; **Accepted**: July 26, 2019; **Published**: August 10, 2019

Abstract: Combined PET/MR is a relatively new technique and so far there has been a very limited report of the potential simultaneous PET/MR and PET/CT application in the evaluation of neuroendocrine tumours. The present study aimed to compare "Ga-DOTATATE PET/CT and PET/MR imaging in patients with known neuroendocrine tumours (NET) and assess the confidence in anatomic lesion detection and localization. We analysed the data of 37 NET patients who underwent both ^{68}Ga-DOTATATE PET/CT and PET/MR using the same injected activity. Visual findings by two observers of the two modalities were recorded. SUV max of both primary tumour and liver lesions for both modalities and PET/MR derived apparent diffusion coefficient (ADC) values were measured. To study the value of additional MRI sequences, the differences in performance between PET with T1+T2w, PET with DWI reads, and PET with post contrast was assessed. No significant differences between the two modalities were seen regarding the number of patients affected by primary or metastatic disease. However, counting the number of lesions per patient, both observers were able to recognize more liver lesions in MRI T1 and T2. The interclass correlation coefficient (ICC) demonstrated a strong correlation between SUV max derived from PET/CT and PET/MR in both primary lesions (ICC = 0.92; p = 0.001) and liver (ICC = 0.882; p = 0.001). In the evaluation of lesion per patient, PET+ contrast and DWI detected more metastasis than the evaluation of PET +T1 and T2 alone. There was no significant correlation between ADC values and PET/MR SUV max of the tumour (respectively: p = 0.43, p 0.88 and p = 0.295). PET/MRI has comparable accuracy in localization and staging to PET/CT, and has a potential to become a valid alternative to PET/CT in staging and follow up of NET patients, with advantages in the characterization of liver lesions. In our study DWI and contrast helped to detect more lesions.

Keywords: PET/MRI, ^{68}Ga-DOTATATE, Neuroendocrine Tumours

1. Introduction

Neuroendocrine tumors (NETs) are a heterogeneous class of relatively rare tumors that is of increasing incidence, of approximately 4 per 100,000 persons per year in the UK [1], possibly reflecting improved diagnostics. These tumors originate from neuroendocrine cells, most commonly from

the gastroenteropancreatic and bronchopulmonary system. An increasing incidence has been observed over the last decades, and disease-free survival is stagnating [2]. Metastatic disease has a high prevalence in this entity, predominantly in gastroenteropancreatic NET. Early diagnosis NET is mandatory for successful treatment, because the size of the primary NET (at least those in the relatively common jejuneal / ileal site) correlates with the occurrence of lymph node involvement [3]. However, the subtle and ambiguous clinical manifestations of NETs can frequently hamper a timely and accurate diagnosis, despite recourse to modern laboratory diagnostics. In particular, elevated levels of Chromogranin A (CgA), which is widely expressed by neuroendocrine cells, give a sensitivity of approximately 70%–85% in patients with known NET. However, elevated CgA is not sufficient for diagnosis, because it can arise from treatment with proton pump inhibitors, atrophic gastritis, renal insufficiency, and numerous other conditions [4-5]. It has been reported that there is the greater expression of somatostatin receptors in high and intermediate histological grades compared with less differentiated forms which have an aggressive course. Chelator-conjugated somatostatin analogs labeled with ^{68}Ga (eg, DOTATATE, DOTANOC, and DOTATOC) due to a high affinity for somatostatin receptors (SSTRs) have an increased diagnostic accuracy over conventional imaging and Octreoscan in several studies [6-7]. Uptake of ^{68}Ga-DOTA peptides is very well correlated to the expression of SSTR type 2 in NETs, in particular, which allows sensitive diagnosis of well-differentiated NETs (G1 and G2) in ^{68}Ga-DOTA peptide PET/CT and quantification of SSTR expression; the latter also enables identification of patients who are eligible for peptide receptor radiotherapy with 177Lu-DOTA peptides [8]. In view of the literature, ^{68}Ga-DOTA peptide PET/CT is currently recommended as the imaging technique of choice by the European Neuroendocrine Tumor Society [9].

In conventional PET/CT scanners, attenuation correction is performed on the basis of a CT scan that is used to generate an attenuation map based on a transformation of the CT Hounsfield units into attenuation factors at the 511 keV. Naturally, the MRI signal does not provide information on the radiodensity of the tissue and cannot directly be used for attenuation correction. Several alternative approaches have been discussed, including anatomically based attenuation maps and automatic atlas-based pattern recognition approaches. The procedure implemented in the Biograph mMR (the system used in this study) uses an MRI-based attenuation map that is generated on the basis of a 2-point Dixon MRI sequence. The Dixon sequence allows estimation of the distribution of 4 different tissue types (fat, soft tissue, lungs, and background/air) throughout the body and the calculation of an attenuation map on the basis of the presumed radiodensity of these tissue types [10-11]. However, so far the quality of clinical PET data acquired on an integrated whole-body PET/MR scanner and attenuation-corrected by means of MRI data has not been systematically compared with PET data acquired on a PET/CT scanner for the same patients.

Within the last few years, integrated PET/MRI scanners have become available for clinical use. While it is unlikely that PET/MRI will replace PET/CT in regular patient workup and clinical routine in the future, PET/MRI has certain advantages that may add useful information, because of the superior soft-tissue contrast of MRI, and furthermore the possibility of obtaining functional information when diffusion-weighted imaging (DWI) or dynamic contrast enhanced imaging with hepatocellular contrast agents for detection of liver metastases is included in the MRI protocol. Nevertheless, in patients with NETs, it is unclear whether ^{68}Ga-DOTANOC PET/MRI is actually superior to ^{68}Ga-DOTANOC PET/CT, because of the high sensitivity (Se) and specificity (Sp) of the radiotracer itself [12]. To our knowledge, so far there has been very limited report of the potential simultaneous PET/MR and PET/CT application of this technique in the evaluation of neuroendocrine tumours. Combined positron emission tomography/magnetic resonance imaging (PET/MR) is a relatively new technique that has shown similar performance to positron emission tomography /computed tomography (PET/CT) in several, but generally small sample size, and inhomogeneous FDG studies [13-15].

The aim of this study was to evaluate the clinical performance (quantitatively and qualitatively) of integrated whole-body ^{68}Gallium-DOTA-Tyr3-Octreotate (^{68}Ga-DOTATATE) PET/MR as compared with whole-body ^{68}Ga-DOTATATE PET/CT in patients with histologically proven neuroendocrine tumours, and to assess the inter-observer agreement in anatomic lesion detection and localization. Moreover, we aimed to assess the role of MR sequences, in addition to PET images, in the evaluation of metastatic disease and also the reliability of anatomic allocation of the suggestive PET findings in PET/MR (by means of the MRI Dixon images) in the entire body in comparing to that of low-dose CT in conventional PET/CT. We hypothesized that ^{68}Ga-DOTATATE PET should detect NET lesions with a high sensitivity in this patient group.

2. Materials and Methods

This study included 37 (20 males and 17 females; mean age: 56.4 years, median 62 years, range 18-82 years) patients that were referred for localizing primary (n=5), initial staging (n=15), restaging and monitoring response to therapy (n=9), and detection of recurrence (n=8). All subjects underwent a single-injected dose of ^{68}Ga-DOTATATE (138-180 MBq; average activity, 150 MBq) and dual-imaging protocol including PET/CT and subsequent PET/MR. All patients had PET/CT before PET/MR and the interval time between the two scans varied from 25 to 40 min depending on patient's mobility. All the data included in the study were collected for clinical purposes, and for the purposes of service development. The retrospective institutional review board approved use of the data.

2.1. Radiation Dose Estimation

FOR ^{68}GA, the actual radiation dose resulting from the ^{68}Ga-DOTATATE PET scan is dependent on the radiopharmaceutical, the injected ^{68}Ga-DOTATATE dose. The effective dose equivalent (whole body) has been estimated to be 0.025 mSv/MBq for adults. The critical organs are spleen, urinary bladder, kidneys and liver; they receive 0.28 mSv/MBq, 0.13 mSv/MBq, 0.09 mSv/MBq, 0.05 mSv/MBq [16] respectively.

2.2. PET/CT Imaging

^{68}Ga-DOTATATE was prepared as per local protocol. Whole-body PET scans were acquired in 3-dimensional mode using a Biograph 64 TruePoint (Siemens Medical Solutions) or a Discovery 64-slice PET/CT scanner (GE Healthcare). The emission recording sequence was initiated 60 min after intravenous injection of 200 MBq of ^{68}Ga-DOTATATE (except 1 child, who received 50 MBq), as in previous studies [17]. Emission data were reconstructed with attenuation correction using concurrent diagnostic CT. Two experienced nuclear medicine specialists evaluated the PET images for the presence or absence of NET by consensus. PET images were evaluated visually for regions of pathologically increased tracer uptake that could not be attributed to normal physiological activity. CT data were used for allocation of regions with increased radiopharmaceutical uptake to specific structures. The readers were aware of the patients' clinical history.

All patients underwent whole-body PET/CT (Discovery VCT; GE Healthcare, Milwaukee, Wisconsin, U.S.A.) from skull vertex to mid-thigh after a single intravenous injection of ^{68}Ga-DOTATATE, accordingly to EANM guidelines. Acquisition began at 45 min after ^{68}Ga-DOTATATE injection. A low dose non-enhanced CT scan was acquired for attenuation correction at 120 keV and mA modulation was employed (smart 30-300 mA, noise index 20, 0.8s rotation, pitch 1.75). PET acquisitions were acquired in 3 dimensions with 9-slice overlaps and 4 min/bed position. The CT images were converted to maps of PET attenuation coefficients using a bilinear transformation based on the use of different scaling factors for materials with Hounsfield units. A 3-dimensional attenuation- weighted ordered-subsets expectation maximization iterative reconstruction algorithm (AW OSEM 3D) was applied to transaxial slices (128x128 matrix, corresponding to a 70-cm-diameter FOV) with 2 iterations; 21 subsets and post processing filter, 5.14 mm.

2.3. PET/MR Imaging

PET/MR imaging was performed using a Siemens 3T Biograph mMR system (Siemens, Erlangen, Germany) with an integrated PET system within the MR gantry, which allows simultaneous PET and MR acquisitions without having to reposition the patient. Total examination time varied between 8 min (1 bed) to 40 min (whole body scan, 5 beds).

The technical specifications have been summarized recently in a performance evaluation paper [18]. In brief, this system consists of a 3-TMRI scanner featuring high performance gradient systems (45mT/m) and a slew rate of 200 T/m/s. The PET/MR system is equipped with Total Imaging Matrix coil technology (Siemens), covering the entire body with multiple integrated radiofrequency surface coils. This technology allows MRI acquisitions of the whole body without the need to interrupt the examination for repositioning of coils for different body regions. Technical details of the PET/MR protocol for this study are listed in Table 1. The PET scanner has a spatial resolution of 4.3 at 1 cm and of 5.0 mm at 10 cm from the transverse FOV and a sensitivity of 15.0 kcps/MBq at the center of the FOV. The axial FOV is 25.8 cm, which allows covering the entire body with a low number of BPs in a short time.

2.4. Imaging Protocol

Patients were positioned in the MRI scanner as similarly as possible to their positioning for the PET/CT examination. The combined PET/MR acquisition was initiated with 1–5 BPs at a 4-min acquisition time per BP. First, a coronal 2-point Dixon 3-dimensional volumetric interpolated breath-hold T1-weighted MRI sequence was acquired at each BP and used for the generation of attenuation maps and for anatomic allocation of the PET results. This approach has recently been demonstrated to provide results comparable to those of conventional attenuation correction by low dose CT [18]. The software of the MRI scanner automatically used the raw images to generate 4 different images: T1-weighted in-phase, T1-weighted out-of-phase, water-only, and fat-only.

Simultaneously with the start of the Dixon MRI sequence, the PET acquisition will start at the same BP, thus ensuring optimal temporal and regional correspondence between MRI and PET data. The PET acquisition time was 4 min per BP, taking delayed acquisition times and radioactive decay into account. In the thorax and abdomen regions, the MRI scans were acquired during breath-hold in shallow inspiration, similar to the acquisition of the low-dose CT. Subsequently, the patients were instructed to continue breathing during the remaining PET acquisition time. Attenuation of the PET signal caused by instrumentation such as the patient bed and the fixed MRI coils is automatically integrated into the attenuation maps. The PET data were reconstructed using ordered-subset expectation maximization with 21 subsets and 3 iterations and a Gaussian filter of 5 mm in full width at half maximum (FOV, 359x 359 mm; 2-mm slice thickness; 127 slices).

Table 1. *Technical details of the PET/MR protocol used during the study.*

Sequence	Orientation	TR	TE1	TE2	Flip Angle	FOV	Matrix	Slice Thickness (mm)
T1 2 point Dixon	Axial/coronal	4.13	1.31	2.54	9°	380x297	320x320	3
T2 Haste	Axial	1500-1800	119	NA	>90°	500x375	448x448	5
T1 vibe post contrast	Axial	4.13	1.31	2.46	9°	500x500	320x320	3
DWI (0,400,800)	Axial	8400	88	NA	NA	282x350	NA	5

2.5. Image Evaluation

PET/MR data were anonymized and sent to a workstation (OsiriX, Pixmeo Sarl, Switzerland; http://www.osirix-viewer.com/) for evaluation. To allow the comparison between PET/CT and PET/MR, the same set of images (with similar anatomical coverage for both modalities) was chosen by a separate nuclear medicine physician who was not involved in the reading. The images were then interpreted by two dual accredited radiologists with nuclear medicine training with dedicated skills in MR and 3 years of experience in PET/MR. Images were initially interpreted separately and then discordant findings, if present, were resolved by consensus. Readers were unaware of the clinical, pathological results and imaging findings of the other modalities. Readers were asked to evaluate, with at least a gap of one day between the different sessions, the following sequences coupled with the PET acquisition: coronal + axial multiple point T1-WI Dixons and T2-WI Haste; T1-WI post contrast; diffusion weighted imaging (DWI) and apparent diffusion coefficient (ADC) map. PET + T1 + T2 were read first then post contrast, DWI, and ADC findings were added later. PET/CT studies were interpreted by a qualified nuclear medicine physician with 4 years' experience. Any localization with an intensity greater than background that could not be explained by physiological uptake was considered to be a positive scan for somatostatin receptor expression. Physiological tracer uptake is normally seen at the pituitary, salivary glands, thyroid, liver, spleen, adrenals, kidneys, ureters, and urinary bladder with the highest uptake seen in the spleen, and the liver showing variable and mild uptake. Pancreatic head uptake similar to the liver was considered physiological. For each lesion, the SUV max was recorded by using an automated volume of interest. The ADC map was reviewed on the same imaging console at the same level of the PET ROI to match the same slice were SUV max was measured on the PET component of the study. Values of ADC mean as the average of ADC of all the pixels within the ROI and ADC maximum and minimum values were generated.

2.6. Statistical Analysis

PET/MR and PET/CT findings were recorded in an electronic database (Microsoft Excel 2008; Microsoft Corporation; Redmond, Washington, U.S.A.) and Statistical Package for Social Science SPSS software package (Statistics 22; IBM Company, Armonk, New York, U.S.A.) was used for statistical analysis. The continuous numbers were expressed as mean ± standard deviation [min-max], categorical data are expressed as number (percentage).

2.7. Image Quality Comparison

Subjective analysis of the image quality of the two modalities was evaluated using an arbitrarily point scale of 1-3 (unacceptable, 1; good, 2; and excellent, 3), based on the experience of the readers in PET, CT and MR images. The final point scale was based on tracer distribution and background, lesion sharpness and diagnostic confidence. Wilcoxon signed-rank test was used to assess differences in image quality scoring between PET/CT and PET/MR.

The number of lesions in different regions of interest (liver, pancreas, lung, bone and lymph nodes) was recorded in separate spreadsheets. To facilitate the visual analysis, we arbitrarily divided patients into two groups according to the number of metastases using a threshold (n) equal or more than 5 or (n) less than 5. For quantitative assessment between the two modalities, the interclass correlation coefficient (ICC) was used to assess inter-modality agreement for SUV max of both primary tumour and liver lesions. Only these two categories (primary and liver) were chosen because the sample size was sufficient for statistical analysis following a power analysis. Inter-observer agreement for PET/MR derived SUV max was also assessed using the intra-class correlation coefficient.

To study the value of additional MRI sequences, differences in performance between the reading sessions in detecting liver and bone metastasis (PET with T1+T2w, PET with DWI, and PET with post contrast) were recorded and analysed using the Friedman test. To study the potential impact on the management, a further sub analysis in patients with less than five metastatic deposits in the same lobe of the liver vs. bipolar lesions (a threshold that our oncologists considered as potentially treatable with surgery) was also performed. The liver was chosen for this analysis as it was the organ most involved with metastasis in our sample. The Spearman rank correlation was used to evaluate the correlation between PET/MR derived SUV max and ADC values. A p-value of < 0.05 was considered statistically significant for all statistical tests.

3. Results

Thirty-two (32/37; 86%) patients presented with known primary tumours: 3/32 (9%) paragangliomas, 8/32 (25%) pancreatic NET, 14/32 (44%) mid gut NET, 6/32 (19%) bronchial carcinoid NET, and 1/32 (3%) mediastinal carcinoid. In the remaining five (14%) cases ^{68}Ga-DOTATATE PET/CT was requested for the localization of an unknown primary. These patients presented with biopsy proven NET metastatic disease, but previous cross sectional

imaging modalities have not been able to identify the primary tumours.

Image quality grading results of PET/MR and PET/CT are given in Table 2. The Wilcoxon signed-rank test demonstrated no statistically significant differences between the two modalities (p=0.18 for observer 1 and p=0.32 for observer 2). Both observers of PET/MR and the PET/CT observer reported 7 (18.9%) negative studies and 30 (81.1%) with evidence of ^{68}Ga -DOTATATE avid lesions. In localizing the primary, both modalities correctly identified the same 12 primary sites out of 16 patients (2 in pancreas, 6 in the bowel, 2 in the lung/bronchus, and 2 in the neck) (Figures 1-2).

Table 2. *Image quality grading results of PET/MR and PET/CT.*

Modality	Unacceptable	Good	excellent
PET/MRI observer 1	1	36	0
PET/MRI observer 2	0	33	4
PET/CT Observer	1	32	4

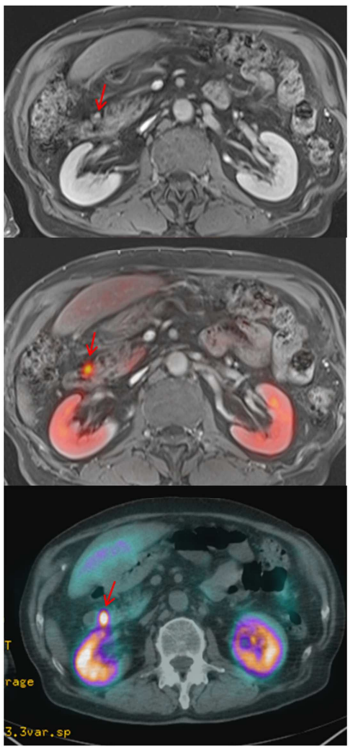

Figure 1. *A 64 years old man with small focus of uptake in the third portion of the duodenum. MR post contrast images clearly shows the enhancing lesion, with corresponding intense uptake at the fused ^{68}Ga Dotatate image (arrows).*

In three patients, referred following histopathology of metastasis and equivocal imaging, with a suspicious pancreatic primary, the diagnosis remained unknown. Multiple follow up scans did not reveal the primary site. In one case, the T1+T2w sequences of MR allowed to differentiate a single focus of uptake in the liver that was considered as metastasis rather than a small primary of the bowel (Figure 3). In another case of vaginal paraganglioma, PET/MR imaging was better in localizing and characterizing the lesions than PET/CT (Figure 2).

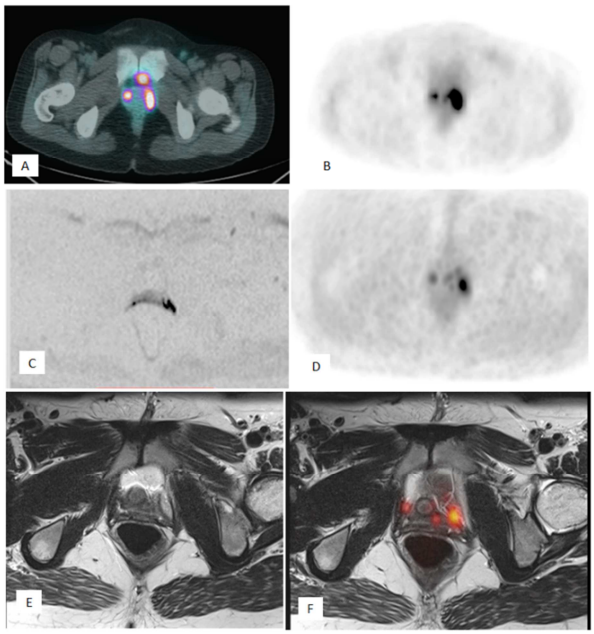

Figure 2. *(A–D) A 16-y-old woman with recurrent multiple vaginal paragangliomas. (A-B) PET-CT show intense uptake around the vaginal walls but no obvious abnormality was seen at the CT component. (C-F) PET-MR allow to exactly localizing the lesions in the lateral upper vaginalwalls. DWI also shows restricted diffusion at the same levels.*

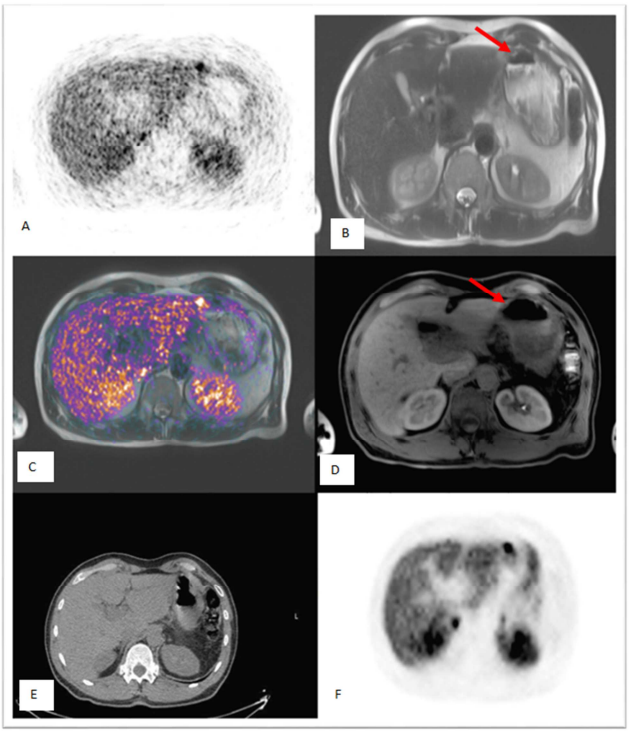

Figure 3. *PET CT and PET MR in a patient with multiple liver lesions. DWI increased the reader ability to characterize a lesion (B) as also seen as a hot spot on the fused PET MR images (D). Corresponding post contrast MR showed no focal lesion at the same level (C). Of note same level PET CT (A) did not show a clear identifiable lesion.*

Nodal and distant disease results are demonstrated in Table 3. Both modalities identified liver metastasis in the same number of patients (n=16).

Table 3. *Nodal and distant disease identified for the both imaging modalities for different anatomical ROI.*

Regions of interest	PET/CT (Lesions- mm)		PET/MRI:T1+T2 (consensus) (Lesions- mm)	
	≥5mm lesion	<5 lesion	≥5 lesion	<5 lesion
Cervical LN	0	0	0	0
Mediastinal LN	1	5	2	4
Abdominal LN	0	10	0	12
Pelvic LN	0	1	0	2
Liver	8	8	14	2
Lung	0	5	0	4
Bone	7	2	5	3

However, counting the number of liver lesions in each patient, both observers were able to recognize more liver lesions in MR (T1 and T2) sequences than CT (Figure 4). On the CT only 8 patients were identified with more than 5 liver lesions, while on the (T1 and T2) MR sequences, 14 patients were recognized. CT was able to identify 5 patients with avid lung lesions while on MR (T1+T2) only 4 cases were identified. In one case a central supra-hilar nodule was erroneously referred as hilar node on PET/MR. More non avid lung lesions were detected by the CT component compared to MRI component (7 lesions versus 4). 12 patients with abdominal lymph nodes were detected on MR (T1 and T2) detected vs 10 patients detected on CT. The ICC demonstrated a strong and statistically significant correlation between the highest SUV max derived from PET/CT and PET/MR in both primary lesions (ICC = 0.92 & p = 0.001) (Figure 5) and liver metastases (ICC = 0.882 & p = 0.001) (Figure 6). Also, the inter-observer agreement for PET/MR SUV max of primary lesions was excellent (ICC = 0.993, p = 0.001).

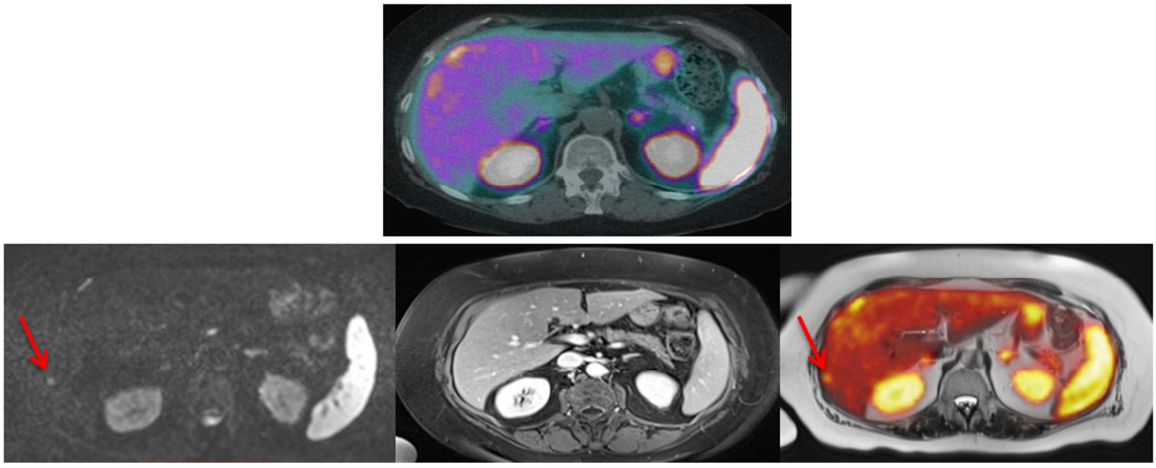

Figure 4. *More liver lesions were observed by the both observes in MR (T1 &T2) sequences than CT.*

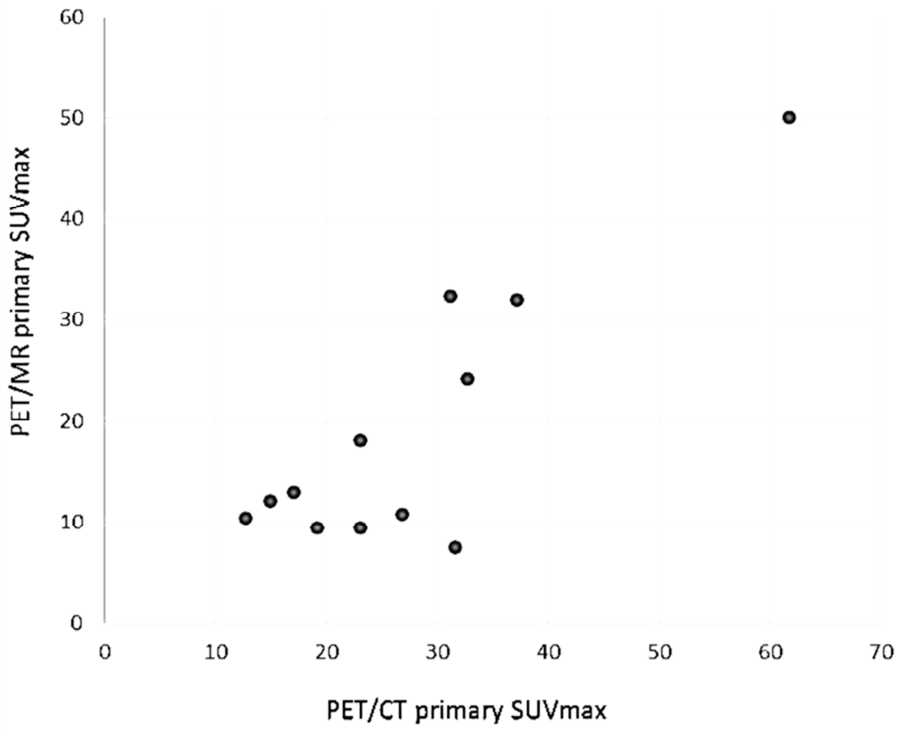

Figure 5. *Excellent inter-modality interclass correlation for SUV max for primary lesions in 12 patients.*

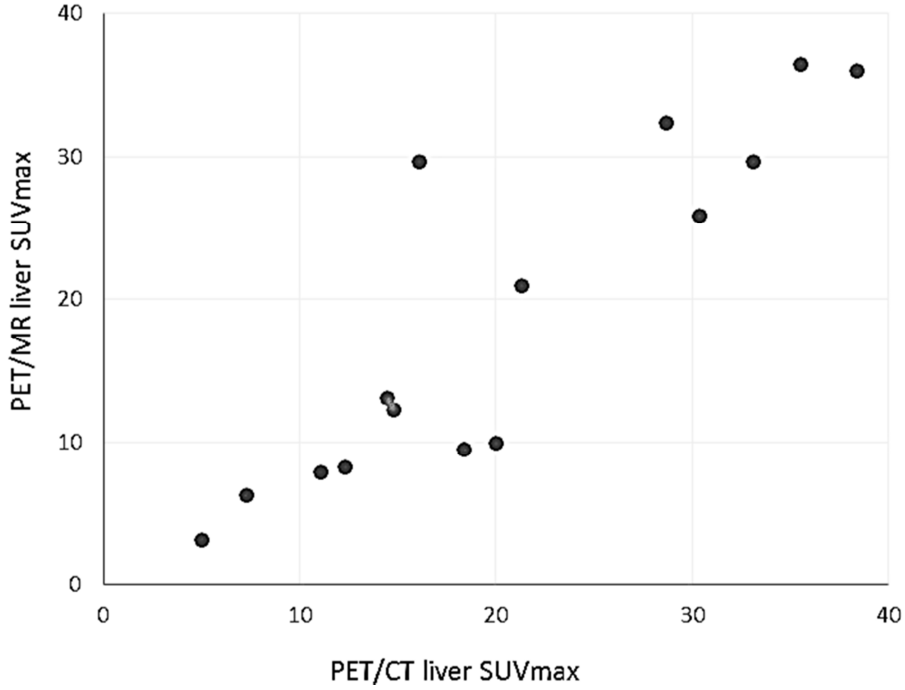

Figure 6. *Excellent inter-modality interclass correlation for SUV max for liver lesions primary lesions in 15 patients (Note: one patient data was not recorded).*

PET with post contrast and PET with DWI reads helped to localize one pancreatic primary, which was initially localized to the pancreatic body on contrast phase then retrospectively on the other sequences. The addition of these sequences to PET also helped to detect more metastatic lesions than PET with T1+T2w alone. For metastatic lesions observer 1 found extra lesions in 6 patients and observer 2 found extra lesions in 10 patients. Table 4 shows the different distribution of the additional metastatic lesions seen by the two observers using DWI and post contrast images in different anatomical regions. This was particularly true when lesions were small in size (average size 8 mm) with low SUV max values (range: 2.8-7). The Friedman test demonstrated that there was not a statistically significant difference between the three reading sessions of PET/MR in the evaluation of liver metastases (0S1 p =0.71; 0S2 p = 0.26) and bone metastases (0S1 p = 0.1; 0S2 p = 0.166). The sub analysis in patients with less than five metastatic deposits in one lobe of the liver confirmed that there was not a statistically significant difference between the reading sessions as well (0S1 p = 0.22; 0S2 p = 0.26). There was no significant correlation between mean, maximum and minimum ADC values and PET/MR derived SUV primary and liver lesions (respectively: p = 0.43, p = 0.88 and p = 0.295).

Table 4. *Ddifferent distribution of the additional metastatic lesions seen by the two observers using DWI and post contrast images in different anatomical regions.*

Organ	liver	lung	bone	LN
Number of lesions on Contrast (observer 1)	2	0	0	3
Number of lesions on DWI (Observer 1)	2	0	1	0
Number of lesions on Contrast (observer 2)	5	2	1	4
Number of lesions on DWI (Observer 2)	1	0	1	2

4. Discussion

This study showed comparable performance of PET/CT and PET/MR (T1 and T2) for the evaluation of NET, with good inter-observer reliability in anatomic lesion localization and quantification with advantages in evaluating liver lesions on T1 and T2 sequences. The number of lesions detected per patient increased by adding the DWI and contrast.

To the best of our knowledge, only one other study has assessed the possible role of PET/MR ^{68}Ga-DOTATATE in histopathological proven NET. Beiderwellen et al [19], in their preliminary experience evaluated a small cohort of 8 patients who underwent ^{68}Ga-DOTATOC PET/CT and a sequential separate day PET/MR study. Similar to our data, they found good inter-observer reliability between both modalities with strong SUV correlation. Nevertheless, so far no complete data are available on the possible application of simultaneous ^{68}Ga-DOTATATE PET /MR in NET patients.

For localizing primary lesions, our study showed that both modalities performed similarly in detecting lesions with PET/MR showing a slight advantage in localizing and characterizing the pancreatic and pelvic lesions due to the better contrast resolution of MR. In the evaluation of lung primary lesions, we found comparable values for both machines in detecting primary lesions. It is of interest that

this is different from the current FDG literature [10, 20-21]; this may be attributed to the intense uptake seen with ^{68}Ga-DOTATATE PET, which overpasses most of the limitations related to the lower resolution of the MR in detecting small lung lesions.

Both modalities initially failed to detect 3 lesions in patients with unknown primary, but on subsequent follow up imaging were found to arise from the pancreas. It is worth to say that detecting primary pancreatic disease has proven to be problematic also in previous PET studies. The physiological "Ga-DOTATATE uptake seen in the uncinated process, related to a higher cellular somatostatin receptor concentration, can lead to misinterpretation of the disease [11, 22]. The added value of more complex MR sequences combined with PET than those used in our study (e.g. dedicated pancreatic protocol, specific MR contrast agents or perfusion imaging), can further improve the assessment of indeterminate pancreatic lesions [13, 23].

In our study both modalities have performed fairly similarly in detecting metastasis with MR (T1 and T2) slightly performing better than CT in detecting the number of liver metastases. This is in agreement with previous studies that demonstrated the limited value of ^{68}Ga-DOTATATE PET/CT in the detection of hepatic metastasis in comparison to contrast enhanced CT and MR which seemed more valuable in this setting [24]. Of note, similar to our study, Beiderwellen and his group [19] found that PET/MR has special advantages in the characterization of liver lesions, specifically adding the DWI sequence. However, they recognized the expected weakness of MRI in the lung and sclerotic bone lesions. In evaluating lung metastatic lesions, we found that PET/MR (T1 and T2) detected 4 out of 5 patients seen on PET/CT. One patient presented with small pulmonary metastasis with mild ^{68}Ga-DOTATATE uptake and this was possibly the reason of the misinterpretation. Other authors recently reported higher nodule detection rate by using Ultrashort Echo Time (UTE) imaging for attenuation correction than dual-echo Gradient echo imaging (68% vs 22%, respectively; P <.001) [23]. Our protocol used 2p Dixon sequences. Since at the time the scans were performed, no validation for the UTE was available yet.

The second question we sought to answer was whether the addition of different sequences might benefit the detection of lesions and follow up of metastatic disease. The reason behind adding the DWI and contrast is to take advantage of the highly vascular nature of NET. With intravenous contrast material, lesions enhance intensely during the arterial phase and wash out during the delayed phase. On the other hand, NET has significantly reduced water diffusion compared with normal tissues. On DWI images, the tumour displays a high signal intensity that can be correlated with other T1- and T2-weighted MR imaging acquisitions for better tumour localization and characterization, thus increasing the reader confidence.

In our study the number of lesions per patient increased by adding the DWI and contrast sequences. This was particularly true for lesions with small size and low SUV values. However, our analysis of the liver and bone metastasis did not yield any statistical difference between the three reading sessions. Therefore, we decided to introduce a threshold of 5 hepatic lesions which was mainly determined by our MDT team as the threshold for surgical treatment decision. However, this did not show statistical significance as well. A different selection of patients, different thresholds for treatment, or randomization of lesions might affect differences in staging provided by the two modalities.

Previous authors reported lack of benefit of DWI in lesion localization in addition to routine PET/MR sequences in a range of tumors [15, 17, 25]. In 25 oncology patients, Buchbender et al [19] identified 49 lesions both with PET/MR alone and the same number with PET/MR combined with DWI and the authors concluded that DWI has to be questioned as a standard tool for whole-body staging in oncologic PET/MR [26]. Nevertheless, it is worth to say that the evaluation of NET with ^{68}Ga-DOTATATE basically reflects the histological grade of the lesion with high accuracy in neoplasms with high somatostatin receptors. The simultaneous multiparametric acquisition with PET/MR may allow for investigating different aspects of the disease, such as the relation between somatostatin receptors, angiogenesis and cellularity. The addition of the extra sequences may be of value in patients with high-grade disease where ^{68}Ga-DOTATATE uptake is less. Of note, PET/MR was highly accepted by the majority of the oncologists and physicians who participate in the multidisciplinary meetings. In addition, the majority of patients accepted with enthusiasm the new scanner with very limited discomfort and this is also in agreement with recent published data [18].

We recognize some limitations, including the potential selection bias introduced by the retrospective nature of this study. We enrolled patients referred to us for the same- day PET/CT and PET/MR imaging with different oncologic applications, including diseases in body regions where MR is already the gold standard and that might be considered difficult to evaluate with PET/CT. However, this study was mainly performed to demonstrate the feasibility of ^{68}Ga-DOTATATE PET/MR in NET. Further prospective studies will be required to investigate more specific benefit in selected body districts and to have a longer follow up of these patients demonstrating the value of the machine versus a true gold standard. There were also study limitations imposed by our institutional review board, which requested that PET/CT studies to be performed first followed by the PET/MR studies. Hence, PET/CT was acquired 45 minutes after tracer administration, in keeping with the recommendations of the EANM. Because of the time required to move patients to the PET/MR scanner, the PET/MR studies were acquired a mean of 30 minutes after PET/CT. Delayed uptake phase PET is reportedly useful for detection or differentiation of liver lesions on F18 FDG PET imaging because of the elevated tumor to background ration as compared with the early normal uptake phase [18]. Regarding ^{68}6a-DOTATATE there is no available literature to evaluate the utility of delayed PET for assessment of patients with liver metastasis from NET. Interestingly, we noted slight differences

in the SUV max of liver NET lesions and background between PET/CT and PET/MR with a small improvement in tumor to liver ratio in PET/MRI. The mechanisms responsible for this improvement can only be postulated with a liver background decrease over time while maintaining elevated lesion uptake. Further studies are necessary to investigate this point, also considering the degradation of images seen in delayed phases.

Finally, we recognize that a potential bias could be raised by the different protocol of acquisition, i.e. comparing the non-enhanced PET/CT with our routine use of PET/MR, which consisted of a large field of view Ti- and T2-weighted sequences, including diffusion imaging, plus a whole-body gadolinium contrast-enhanced T1-weighted MR, combined after the PET acquisition in an attempt to reproduce a 'diagnostic MR protocol'.

5. Conclusion

In this study, we demonstrated that PET/MR could be an alternative to PET/CT in staging and follow up of patients with NET with some advantages in the characterization of liver lesions. PET/MR allows an opportunity for numerous MRI sequences to be acquired for diagnostic purposes. At the most basic level, the MRI component can provide anatomic localization of ^{68}Ga-DOTATATE uptake in a similar way to PET/CT but there is potential for more advanced, functional sequences to improve upon PET/CT in lesion detection. In our study, DWI and contrast helped to detect more lesions, but other MRI sequences e.g. STIR for bone marrow involvement or dedicated sequences for lung are yet to be investigated. Given the inherent benefits of ionizing radiation dose reduction, and the fact that patients will often require multiple scans, PET/MR has the potential to become part of routine neuroendocrine imaging.

Conflict of Interest and Funding

The authors declare that they have no competing interests.

Informed consent was obtained from all individual participants included in the study.

This article does not contain any studies with animals performed by any of the authors. All procedures performed in studies involving human participants were in accordance with the ethical standards of the institutional and/or national research committee and with the 1964 Helsinki Declaration and its later amendments or comparable ethical standards.

This work was taken at UCLH/UCL-UK which received a proportion of funding from the Department of Health' s NIHR Biomedical Centres funding scheme.

Acknowledgements

We would like to acknowledge Dr. Guillaume Nicolas for his contribution in drafting the manuscript.

References

[1] Ellis L, Shale M, Coleman M P. Carcinoid Tumors of the Gastrointestinal Tract: Trends in Incidence in England since 1971. *The American Journal of Gastroenterology.* 2010; 105: 25632569.

[2] Hallet J, Law CH, Cukier M, et al. Exploring the rising incidence of neuroendocrine tumors: a population-based analysis of epidemiology, metastatic presentation, and outcomes. Cancer. 2015; 121: 589–597.

[3] Jann H, Roll S, Couvelard A, et al. Neuroendocrine tumors of mid-gut and hindgut origin: tumor-node-metastasis classification determines clinical outcome. Cancer. 2011; 117: 3332–3341.

[4] Berzaczy D, Giraudo C, Haug AR, Raderer M, Senn D, Karanikas G, et al. Whole-Body ^{68}Ga-DOTANOC PET/MRI Versus ^{68}Ga-DOTANOC PET/CT in Patients With Neuroendocrine Tumors A Prospective Study in 28 Patients. Clinical Nuclear Medicine. 2017; 42 (9): 669-674.

[5] Ramage JK, Ahmed A, Ardill J, Bax N, Breen DJ, Caplin ME, Corrie P, Davar J, Davies A H, V Lewington V, Meyer T, Newell-Price J, et al. UK and Ireland Neuroendocrine Tumour Society. Guidelines for the management of gastroenteropancreatic neuroendocrine (including carcinoid) tumours (NETS). Gut. 2012; 61 (1): 6-32.

[6] Mojtahedi A, Thamake S, Tworowska I, et al. The value of (68) Ga-DOTATATE PET/CT in diagnosis and management of neuroendocrine tumors compared to current FDA approved imaging modalities: a review of literature. Am J Nucl Med Mol Imaging. 2014; 4: 426–434.

[7] Haug AR, Cindea-Drimus R, Auernhammer CJ, et al. The role of ^{68}Ga-DOTATATE PET/CT in suspected neuroendocrine tumors. J Nucl Med. 2012; 53: 1686–1692.

[8] HaugAR, Assmann G, Rist C, et al. Quantification of immunohistochemical expression of somatostatin receptors in neuroendocrine tumors using ^{68}Ga-DOTATATE PET/CT. Radiologe. 2010; 50: 349–354.

[9] Niederle B, Pape UF, Costa F, et al. ENETS consensus guidelines update for neuroendocrine neoplasms of the jejunum and ileum. Neuroendocrinology. 2016; 103: 125–138.

[10] Yoon SH, Goo JM, Lee SM, Park CM, Cheon GJ. PET/MR Imaging for Chest Diseases: Review of Initial Studies on Pulmonary Nodules and Lung Cancers. Magn Reson Imaging Clin N Am. 2015; 23 (2):245-59.

[11] Krausz Y, Rubinstein R, Appelbaum L, Mishani E, Orevi M, Fraenkel M, et al. Ga-68 DOTA-NOC uptake in the pancreas: pathological and physiological patterns. Clin Nucl Med. 2012; 37 (1): 57-62.

[12] Frilling A, Modlin IM, Kidd M, et al.; Working Group on Neuroendocrine Liver Metastases. Recommendations for management of patients with neuroendocrine liver metastases. Lancet Oncol. 2014; 15: e8–e21.

[13] Vercher-Conejero JL, Paspulati RM, Kohan A, Rubbert C, Partovi S, Ros P, et al. Imaging Pancreatic Pathology with PET/MRI: A Pictorial Essay. Annual Meeting of the Radiological Society of North America. 2013.

[14] Sekine T, Barbosa FG, Sah BR, et al. PET/MR outperforms PET/CT in suspected occult tumors. Clin Nucl Med. 2017; 42: e88–e95.

[15] Xie P, Liu K, Peng W, Zhou Z. The Correlation between Diffusion-Weighted Imaging at 3T Magnetic Resonance Imaging and Histopathology for Pancreatic Ductal Adenocarcinoma. J Comp Assist Tomogr. 2015; 39 (5): 697-701.

[16] Flechsig P, Zechmann CM, Schreiweis J, Kratochwil C, Rath D, Schwartz LH, et al. Qualitative and quantitative image analysis of CT and MR imaging in patients with neuroendocrine liver metastases in comparison to ^{68}Ga-DOTATOC PET. Eur J Radiol. 2015; 84 (8): 1593-600.

[17] Noij DP, Pouwels PJ, Ljumanovic R, Knol DL, Doornaert P, de Bree R, et al. Predictive value of diffusion-weighted imaging without and with including contrast-enhanced magnetic resonance imaging in image analysis of head and neck squamous cell carcinoma. Eur J Radiol. 2015; 84 (1): 108-16.

[18] Shortman RI, Neriman D, Hoath J, Millner L, Endozo R, Azzopardi G, et al. A comparison of the psychological burden of PET/MRI and PET/CT scans and association to initial state anxiety and previous imaging experiences. Br J Radiol. 2015; 88: 20150121.

[19] Beiderwellen K, Poeppel T, Hartung-Knemeyer V, Buchbender C, Kuehl H, Bockisch A, et al. Simultaneous ^{68}Ga-DOTATOC PET/MRI in patients with gastroenteropancreatic neuroendocrine tumors: initial results. Invest Radiol. 2013; 48 (5): 273-279.

[20] Stolzmann P, Veit-Haibach P, Chuck N, Rossi C, Frauenfelder T, Alkadhi H, et al. Detection rate, location, and size of pulmonary nodules in trimodality PET/CTMR: comparison of low-dose CT and Dixon- based MR imaging. Invest Radiol. 2013; 48 (5): 241-246.

[21] Ohno Y, Koyama H, Yoshikawa T, Takenaka D, Seki S, Yui M, et al. Three-way Comparison of Whole-Body MR, Co-registered WB FDG PET/MR, and Integrated Whole-Body FDG PET/CT Imaging: TNM and Stage Assessment Capability for Non-Small Cell Lung Cancer Patients. Radiology. 2015; 275 (3): 849-61.

[22] Jacobsson H, Larsson P, Jonsson C, et al. Normal uptake of ^{68}Ga-DOTA-TOC by the pancreas uncinate process mimicking malignancy at somatostatin receptor PET. Clin Nucl Med. 2012; 37: 362-365.

[23] Etchebehere EC, de Oliveira Santos A, Gumz B, Vicente A, Hoff PG, Corradi G, et al. ^{68}Ga-DOTATATE PET/CT, 99mTc-HYNIC Octreotide SPECT/CT, and Whole-Body MR Imaging in Detection of Neuroendocrine Tumors: A Prospective Trial. Nucl Med. 2014; 55: 1598-1604.

[24] Schreiter NF, Nogami M, Steffen I, Pape UF, Hamm B, Brenner W, R6ttgen R. Evaluation of the potential of PET/MRI fusion for detection of liver metastases in patients with neuroendocrine tumours. Eur Radiol. 2012; 22 (2): 458-67.

[25] Flechsig P, Zechmann CM, Schreiweis J, Kratochwil C, Rath D, Schwartz LH, et al. Qualitative and quantitative image analysis of CT and MR imaging in patients with neuroendocrine liver metastases in comparison to ^{68}Ga-DOTATOC PET. Eur J Radiol. 2015; 84 (8): 1593-600.

[26] Buchbender C, Hartung-Knemeyer V, Beiderwellen K, Heusch P, Kuhl H, Lauenstein TC, et al. Diffusion-weighted imaging as part of hybrid PET/MR' protocols for whole-body cancer staging: Does it benefit lesion detection? European Journal of Radiology. 2013; 82: 877-882.